



Cite this: DOI: 10.1039/c5nj01153a

# A novel water-soluble hydrophobically associating polyacrylamide based on oleic imidazoline and sulfonate for enhanced oil recovery†

 Shaohua Gou,<sup>\*ab</sup> Shan Luo,<sup>b</sup> Tongyi Liu,<sup>b</sup> Peng Zhao,<sup>b</sup> Yang He,<sup>b</sup> Qinglin Pan<sup>b</sup> and Qipeng Guo<sup>\*c</sup>

3-(2-(2-Heptadec-8-enyl-4,5-dihydro-imidazol-1-yl)ethylcarbamoyl)acrylic acid (NIMA), 3-(diallyl-amino)-2-hydroxypropyl sulfonate (NDS), acrylamide (AM) and acrylic acid (AA) were successfully utilized to prepare novel acrylamide-based copolymers (named AM/AA/NIMA and AM/AA/NDS/NIMA) which were functionalized by a combination of imidazoline derivative and/or sulfonate *via* redox free-radical polymerization. The two copolymers were characterized by infrared (IR) spectroscopy, <sup>1</sup>H nuclear magnetic resonance (<sup>1</sup>H NMR), viscosimetry, pyrene fluorescence probe, thermogravimetry (TG) and differential thermogravimetry (DTG). As expected, the polymers exhibited excellent thickening property, shear stability (viscosity retention rate 5.02% and 7.65% at 1000 s<sup>-1</sup>) and salt-tolerance (10 000 mg L<sup>-1</sup> NaCl: viscosity retention rate up to 17.1% and 10.2%) in comparison with similar concentration partially hydrolyzed polyacrylamide (HPAM). The temperature resistance of the AM/AA/NDS/NIMA solution was also remarkably improved and the viscosity retention rate reached 54.8% under 110 °C. According to the core flooding tests, oil recovery could be enhanced by up to 15.46% by 2000 mg L<sup>-1</sup> of the AM/AA/NDS/NIMA brine solution at 80 °C.

Received (in Victoria, Australia)  
7th May 2015,

Accepted 7th July 2015

DOI: 10.1039/c5nj01153a

www.rsc.org/njc

## Introduction

With the developments in exploring complicated geologic reservoirs, increasing attention has been paid to maximizing the residual oil obtained, which was retained in the formation after water flooding.<sup>1,2</sup> Generally, polyacrylamide (PAM) and/or partially hydrolyzed polyacrylamide (HPAM), as the most commonly utilized water-soluble polymers in commercial chemical EOR applications,<sup>3–6</sup> impair the viscosity in high-salinity environments and deform extremely at high-temperature.<sup>7–9</sup> Furthermore, the thickening power is greatly reduced at an elevated shear rate and shear stress, which is associated with the irreversible shear degradation of their linear flexible chains.<sup>10–12</sup>

Recently, hydrophobically associating polymers (HAPAM), where PAM is modified with a small number of various hydrophobic groups, have been proposed for use as oil-field chemical additives by many researchers,<sup>13–16</sup> which can somewhat improve linear flexible chains as a means to preferably resist harsh formation conditions. Numerous research efforts have confirmed that hydrophobic moieties incorporated directly into the backbone of polymers are associated in the aqueous phase by intra and intermolecular interactions once above the critical micelle concentration.<sup>17–19</sup> Owing to the reversible dissociation process of physical links, those proved the distinct shear thinning and thixotropy in aqueous solutions under shear rate and shear time. Additionally, the high surface and interfacial activities exhibited by most hydrophobic moieties on functionalized polymers were found to be related to the presence of hydrophobic groups.<sup>20–22</sup> Commercially, given particular rheological properties, high surface and interfacial activities, the potential of those polymers in EOR applications has been of great interest in chemical technology for use in surfactant chemistry,<sup>16</sup> flocculation,<sup>15</sup> profile modification,<sup>23,24</sup> and as industrial thickeners,<sup>25</sup> *etc.*

The solubility of hydrophobically associating polymers in aqueous phase, one of the most considerable requirements in the process of oil exploration, therefore, has been given increasing attention. However, HAPAM implemented in many oil applications,

<sup>a</sup> State Key Laboratory of Oil and Gas Reservoir Geology and Exploitation, Southwest Petroleum University, Chengdu, Sichuan 610500, China.

E-mail: shaohuagou@swpu.edu.cn

<sup>b</sup> Oil & Gas Field Applied Chemistry Key Laboratory of Sichuan Province, College of Chemistry and Chemical Engineering, Southwest Petroleum University, Chengdu, Sichuan 610500, China

<sup>c</sup> Polymers Research Group, Institute for Frontier Materials, Deakin University, Locked Bag 20000, Geelong, Victoria 3220, Australia. E-mail: qguo@deakin.edu.au

† Electronic supplementary information (ESI) available: Synthesis routes, and their initial <sup>1</sup>H NMR spectrogram analysis of NDS and NIMA; solution preparation and characterization; fluorescence spectra of different concentrations of copolymer solutions; the composition of synthesized brine for dissolving polymer particle samples in the rheological experiments. See DOI: 10.1039/c5nj01153a

even in laboratory study, has been demonstrated to incompletely disperse in aqueous phase.<sup>26–28</sup> Compared with conventional water-soluble polymers, HAPAM presents poor dissolving capacity with the increase in hydrophobic moieties.<sup>29–32</sup> In parallel with the ongoing discussions on the contribution of hydrophobic long chains to the relative poor solubility of HAPAM, other acrylamide-based polymers functionalized with efficient comonomers have been extensively reported in the literature in a bid to improve their water solubility and oilfield chemical applications; for instance, the combination of acrylamide with sulfonamide groups,<sup>33–35</sup> sulfonic acid groups,<sup>36,37</sup> phosphate groups,<sup>38</sup> zwitterion groups<sup>39,40</sup> and others exhibited a more preferable hydrolysis ability in the application process for EOR.

In this article, we had hierarchically synthesized the monomer, namely, 3-(2-(2-heptadec-8-enyl-4,5-dihydro-imidazol-1-yl)ethyl-carbamoyl)acrylic acid (NIMA) with an imidazoline ring structure in conjunction with a long aliphatic chain hydrophobic moiety, and the other one, denoted as 3-(diallyl-amino)-2-hydroxypropyl sulfonate (NDS) with a sulfonate group. Then, the novel water-soluble polymers (named as AM/AA/NIMA and AM/AA/NDS/NIMA, respectively), found to be composed of acrylamide (AM), acrylic acid (AA), NIMA and/or NDS, were synthesised *via* a simple free-radical co-polymerization strategy. Infrared spectroscopy (IR), <sup>1</sup>H nuclear magnetic resonance (<sup>1</sup>H NMR), thermogravimetry (TG), differential thermogravimetry (DTG), viscosimetry, and the use of a pyrene fluorescence probe were conducted to characterize the morphologies for the obtained polymers. The polymers were placed in aqueous solution or brine, whereupon we further focused our research of the influence of their environments on their unique properties for EOR, such as thickening ability, dissolving capacity, thermal stability, anti-shear degradation, rheological behavior, salt tolerance, resistance factor, residual resistance factor, and EOR value.

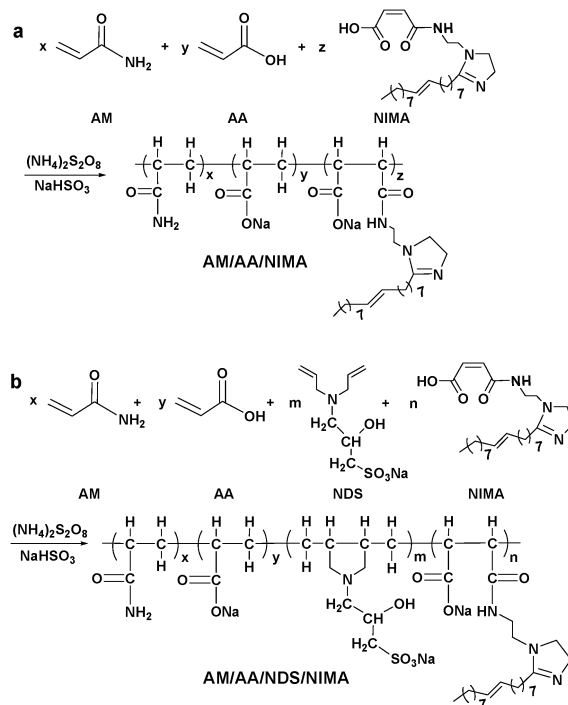
## Experimental section

### Materials

Acrylamide (AM), acrylic acid (AA), sodium bisulfite (NaHSO<sub>3</sub>), ethanol, sodium hydroxide, ammonium persulfate ((NH<sub>4</sub>)<sub>2</sub>S<sub>2</sub>O<sub>8</sub>), maleic anhydride (MA), oleic acid, diethylenetriamine, epichlorohydrin, and diallyl amine were all of analytical reagent grade and were used directly without further purification treatment. The above chemicals were purchased from Kelong Chemical Reagent Factory (Chengdu, China). The partially hydrolyzed polyacrylamide (HPAM) had a 20–30% degree of hydrolysis,  $M_w = 5 \times 10^6$ . The reservoir-simulating brine used in this paper was prepared with the inorganic salt on the basis of most formation reservoirs, such as NaCl, KCl, CaCl<sub>2</sub>, NaHCO<sub>3</sub>, Na<sub>2</sub>SO<sub>4</sub>, and MgCl<sub>2</sub>·6H<sub>2</sub>O, *etc.*

### Synthesis

**Preparation of functionalized comonomers.** See the ESI† for the detailed synthesis procedure and synthesis routes of the comonomers NIMA and NDS. Furthermore, the detailed characterization of NIMA and NDS are given in the ESI.†



Scheme 1 Synthesis routes of (a) AM/AA/NIMA and (b) AM/AA/NDS/NIMA.

**Synthesis of copolymers AM/AA/NIMA and AM/AA/NDS/NIMA.** The indicated amounts of raw materials AM, AA, NIMA and/or NDS were added into a flask with mechanical stirring in deionized water under an inert nitrogen atmosphere. NaOH solution was utilized to regulate the pH to a given value with magnetic stirring for 10–15 min. Copolymerization was allowed to initiate by the addition of (NH<sub>4</sub>)<sub>2</sub>S<sub>2</sub>O<sub>8</sub> and NaHSO<sub>3</sub> (molar ratio 1 : 1) at a stated temperature for a minimum of 6 h. The white granular copolymers, after being purified repeatedly through ethanol, were dried at 45–55 °C under vacuum for approximately 8–12 h. The synthesis routes were shown in Scheme 1.

### Pyrene fluorescence probe

The fluorescence intensities were measured with a Shimadzu RF-5301PC spectrofluorophotometer with excitation at 335 nm. A slit width of excitation and emission was fixed at 5 nm and a spectral range was scanned at 350–580 nm with a temperature of 25 °C. The different concentration copolymer solutions were prepared with the saturated aqueous solution of pyrene; the concentration of pyrene was about  $2 \times 10^{-6}$  mol L<sup>-1</sup>.<sup>41</sup> The ratios between the strength of the first peak ( $I_1$ ) and the third peak ( $I_3$ ) in the fluorescence spectra were calculated.

### Water solubility test

The solution conductivity was measured by using a DDS-11A conductivity meter (Shanghai Rex Xinjing Instrument Co., Ltd, China). Polymer particle samples (16–20 meshes) were dispersed and dissolved in deionized water performing at the ambient temperature (about 25 °C). The water solubility curves

were obtained using the dissolution time, which is defined as the time from initially adding the polymer to the solution conductivity stabilizing.

### Rheological characterization

The rheological behaviors were measured with an advanced polymer analyzer (Haake RheoStress 6000 rotational rheometer) from Germany. Shear-tolerance measurements were investigated with a shear rate ranging from 7.34 to 1000 s<sup>-1</sup> under a constant temperature of 30 °C. Shear recovery performance measurements were carried out using an alternate shear rate between 170 s<sup>-1</sup> and 510 s<sup>-1</sup> at a desired concentration at 30 ± 1 °C. Temperature-resistance tests were conducted by varying the temperature from 25 °C to 120 °C under a shear rate of 170 s<sup>-1</sup>. The total salinity of the synthetic brine across the rheological tests was about 3500 mg L<sup>-1</sup> (see Table S1, ESI<sup>†</sup>). The polymer solutions were kept stationary to temperature equilibrate for a minimum of 15 min before characterisations were carried out to guarantee that the experiments are mainly accurate. The viscoelastic measurement was carried out with the oscillatory frequency ranging from 0.01 to 10.00 Hz at the steady-state stress under 30 °C.

### Core flooding test

A series of one-dimensional sand-packed models were utilized to test the effect of the copolymers on enhanced oil recovery by the combination of saturated brine/polymer flooding at 80 °C. The simulated oil (67.4 mPa s at 80 °C) was prepared as the oil phase in the core flooding experiments. The water-flooding across the core plugs was prepared in advance by dissolving different salts in deionized water so that the total salinity was about 7200 mg L<sup>-1</sup> (see Table 1). To eliminate capillary side effects, all flooding experiments were performed at an original flow rate of 0.2 mL min<sup>-1</sup>, afterwards elevated to 0.5 mL min<sup>-1</sup>.

The experiment involved following steps: (1) the simulated crude oil was placed so as to infuse the prepared core assembly, wherein the sand was dry for a minimum of 24 hours before performing the experiment; (2) at a flow rate of 0.5 mL min<sup>-1</sup>, saline solution was injected to substitute the simulated crude oil until no more oil was produced and the water content was about 95%, wherein the permeability and porosity of the core plugs were estimated by the procedure of replacing the simulated oil; (3) the predissolved copolymer or HPAM solutions were injected to displace the saline water until the pressure difference across the cores was stabilized and no more oil was produced; (4) the subsequent flooding water was eventually injected to replace the above mentioned polymer solution samples until no more oil was produced and the pressure difference for the cores was primarily steady-going.

Table 1 Composition of synthetic water flooding

Ion	Na <sup>+</sup>	K <sup>+</sup>	Ca <sup>2+</sup>	Mg <sup>2+</sup>	Cl <sup>-</sup>	HCO <sub>3</sub> <sup>-</sup>	SO <sub>4</sub> <sup>2-</sup>	Total
Concentration (mg L <sup>-1</sup> )	2231	70	95	226	4026	28	549	7225

## Results and discussion

The AM/AA/NIMA and AM/AA/NDS/NIMA acrylamide-based polymers were prepared *via* redox free-radical polymerization of AM, AA, NIMA and/or NDS in the presence of (NH<sub>4</sub>)<sub>2</sub>S<sub>2</sub>O<sub>8</sub>-NaHSO<sub>3</sub>. After purification and drying, the viscosities of the polymer solutions with the desired concentrations were measured under different conditions.

### Optimal synthesis conditions of copolymerization

The variation in the apparent viscosity of the copolymer solutions (1000 mg L<sup>-1</sup>) with different synthesis conditions was identified by a single variable method, which was measured by a Brookfield DV-III+Pro Viscometer at room temperature (30 °C), as shown in Fig. 1a–e. It was found that the optimal synthesis conditions for the copolymer AM/AA/NIMA were as follows: the initiator concentration was 0.5 wt%; pH value of the solution was 7; the reaction temperature was 40 °C; the ratio of AM and AA in weight was 70:30; loading of NIMA was 1.5 wt%. Then the results of the copolymer AM/AA/NDS/NIMA solution revealed that the maximum apparent viscosity was 379.2 mPa s at 1000 mg L<sup>-1</sup>, in the following conditions: the initiator concentration was 0.5 wt%, pH value of the solution was 7, the reaction temperature was 35 °C, the ratio of AM and AA in weight was 65:35, the concentrations of monomer NDS and NIMA were 2.0 wt% and 1.5 wt%, respectively.

The thickening abilities of the obtained polymers were confirmed under different magnifications at around 30 °C in comparison to HPAM. The apparent viscosity increased in stages along with a strong increase in copolymer concentration in the range of 100–5000 mg L<sup>-1</sup> in aqueous phase. The result demonstrated that the copolymers exert a better thickening property than HPAM (Fig. 1(f)). From the curves of viscosity variation of the copolymers AM/AA/NIMA and AM/AA/NDS/NIMA, a dramatic increase was detected beyond the concentration of 800 mg L<sup>-1</sup> and 1000 mg L<sup>-1</sup>, respectively. This revealed that the catastrophe points of the obtained polymers are lower than that of HPAM. This phenomenon could be induced by the strong interchain association and lead to the formation of large aggregates as the polymer concentration increased and surpassed its critical level. The high-effect thickening behavior of these associative polymers contributed significantly to the network structures of the polymer chains.

### Characteristic analysis

**IR analysis.** The structures of the obtained monomers and copolymers were investigated using an infrared spectrometer, as described in Fig. 2. The copolymers' IR spectra show that the monomers NIMA and/or NDS were successfully introduced into the backbone of the PAM molecular chains on account of the characteristic peaks at 3423 cm<sup>-1</sup>, 1633 cm<sup>-1</sup>, 1540 cm<sup>-1</sup>, 1496 cm<sup>-1</sup>, and 1401 cm<sup>-1</sup> in the AM/AA/NIMA IR spectrum and 3431 cm<sup>-1</sup>, 1673 cm<sup>-1</sup>, 1559 cm<sup>-1</sup>, 1458 cm<sup>-1</sup>, 1400 cm<sup>-1</sup>, 1172 cm<sup>-1</sup>, and 1118 cm<sup>-1</sup> in the IR spectrum of polymer AM/AA/NDS/NIMA. Obviously, the new absorption peaks at around 1172 cm<sup>-1</sup> and 1118 cm<sup>-1</sup> in the AM/AA/NDS/NIMA IR spectrum were attributable to the stretching vibration of

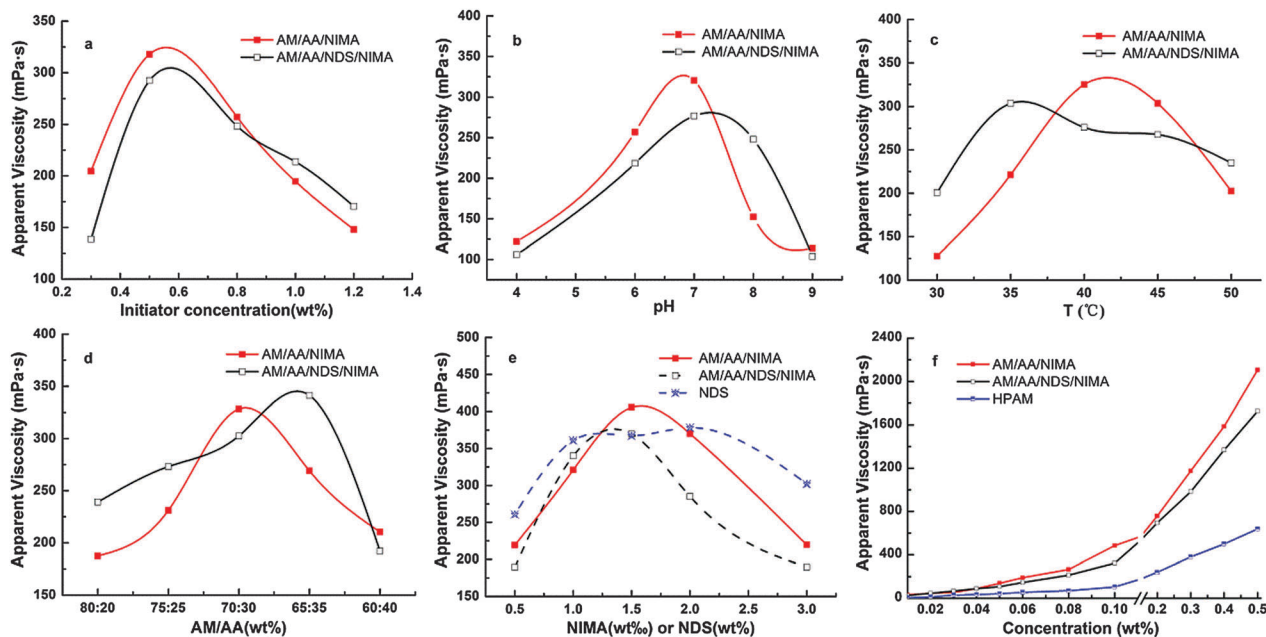


Fig. 1 Effect of (a) initiator concentration, (b) pH, (c) temperature, (d) AM/AA and (e) NIMA or NDS on apparent viscosity for the polymers; (f) the thickening abilities of polymer solutions.

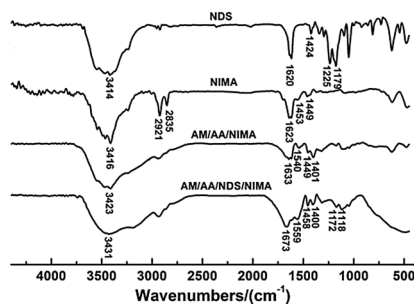


Fig. 2 IR of obtained monomers and copolymers.

$-\text{SO}_3^-$  groups, which belong to the bands at  $1179\text{ cm}^{-1}$  and  $1225\text{ cm}^{-1}$  of  $-\text{SO}_3^-$  groups in the NDS IR spectrum.

**$^1\text{H}$  NMR analysis.** From the  $^1\text{H}$  NMR spectrum of copolymer AM/AA/NIMA in Fig. 3(a), the chemical shift value observed at 7.66 ppm is assigned to the NH protons of  $[\text{CONHCH}_2-]$ . The chemical shift value owing to the NH protons of  $[\text{CONH}_2]$  is observed at 6.84 ppm. The chemical shift value at 5.71–5.73 ppm is attributed to  $-\text{NCH}_2-$  of  $[(\text{CH}_2)\text{NCH}_2\text{CH}_2\text{N}=\text{}]$  of the heterocycle of NIMA. The characteristic peak due to  $-\text{CH}_2\text{N}=\text{}$  of the imidazoline ring was detected at 3.52–3.71 ppm. The chemical shift value around 5.53–5.56 ppm is the protons of the aliphatic  $-\text{CH}=\text{CH}-$  of  $[-\text{CO}(\text{CH}_2)_7\text{CH}=\text{CH}(\text{CH}_2)_7\text{CH}_3]$ , indicating the successful copolymerisation of the NIMA monomer. The chemical shift value at about 1.06–1.07 ppm was attributed to the  $-\text{CH}_3$  proton of the aliphatic chain. The protons of the aliphatic  $-\text{CH}_2-$  and polymeric chain appeared at 1.52 ppm, and the signals of the  $-\text{CH}-$  protons of the polymeric chain were observed at 1.98–2.34 ppm.

Depicted in Fig. 3(b) is the  $^1\text{H}$  NMR spectrum of copolymer AM/AA/NDS/NIMA, which revealed similar morphological

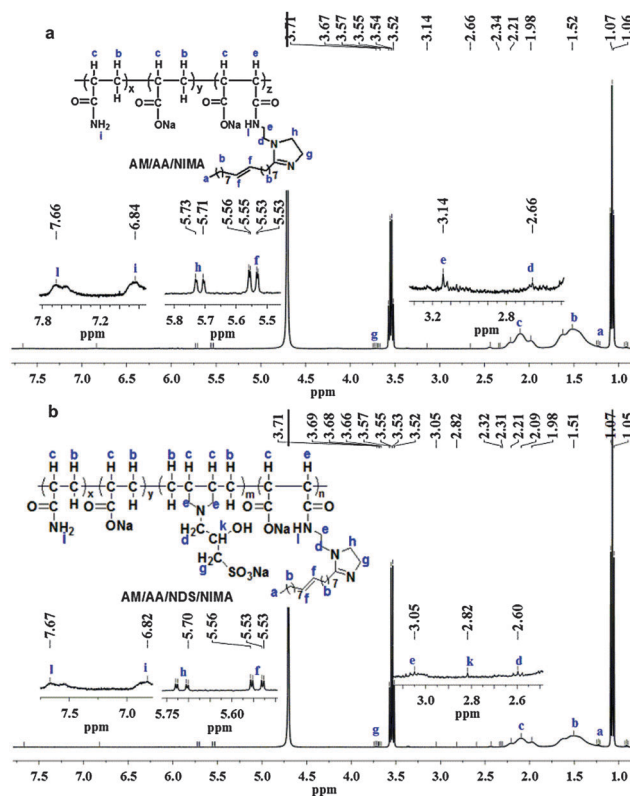


Fig. 3  $^1\text{H}$  NMR of copolymers (a) AM/AA/NIMA and (b) AM/AA/NDS/NIMA.

characteristics to AM/AA/NIMA. The extra peak at 2.82 ppm representing the  $-\text{CH}-$  protons of  $[-\text{CH}_2\text{CH}(\text{OH})\text{CH}_2\text{SO}_3\text{Na}]$ , obviously suggests that the monomer NDS (see Fig. S1 for the  $^1\text{H}$  NMR spectrum, ESI†) was successfully polymerized.

Owing to the synthesis method using NaOH solution to adjust the pH value across the polymerisation reaction, the  $-OH$  protons of  $[-COOH]$  could not be detected.

### Critical association concentration

The ratios ( $I_1/I_3$ ) of the intensities of the first and the third peaks in the pyrene probe fluorescence spectrum (called the "polarity scale") were employed to characterize the critical association concentration (CAC) of the two copolymers, which is defined as the concentration at which the intramolecular association begins to transfer into intermolecular association.<sup>42</sup> The values of  $I_1/I_3$  dependent on concentrations of the copolymers in the fluorescence spectra (see Fig. S2, ESI†) are given in Fig. 4. For the curves of  $I_1/I_3$ , the  $I_1/I_3$  values decreased abruptly when the concentrations of polymers AM/AA/NIMA and AM/AA/NDS/NIMA surpassed  $0.8 \text{ g L}^{-1}$  and  $1.0 \text{ g L}^{-1}$ , respectively. This indicated the formation of a strongly hydrophobic microdomain due to the intermolecular association, and pyrene molecules transferred into the hydrophobic microdomains, giving rise to the abrupt decrease of  $I_1/I_3$  values owing to the weakening polarity of the microenvironment around the pyrene molecule. The results also obviously reveal the relationship curves between the viscosity and polymer concentrations in Fig. 1(f).

### Water solubility

The displacement system, generally, is prepared by injecting water into the oil reservoir in many oilfield applications. The solubility of the water-soluble hydrophobic associating polymer may decline with the increase in hydrophobic moieties however, to restrict the application benefit and formation damage. HAPAM, reported in many articles and numerous experimental studies, can increase significantly the viscosity and weaken the solubility of a polymer, especially at high overall hydrophobic concentrations. Thereby, the solubility of polymers, a crucial factor, should be of concern in the displacement system for EOR.

Presented in Fig. 5 are the conductivity changes in the dissolution process. The solubility of the obtained polymers was more prominent than the common hydrophobic associating polymer, and AM/AA/NDS/NIMA required 63 min to dissolve which was shorter than that of AM/AA/NIMA (92 min). Through an attempt with the water-soluble polymers functionalized on the monomer NIMA with  $-COO^-$  and/or the sulfonate group of NDS, we found that the presence of these groups could slow the

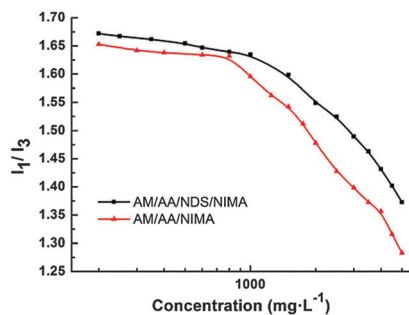


Fig. 4 Effect of different concentrations of copolymers on the  $I_1/I_3$  value.

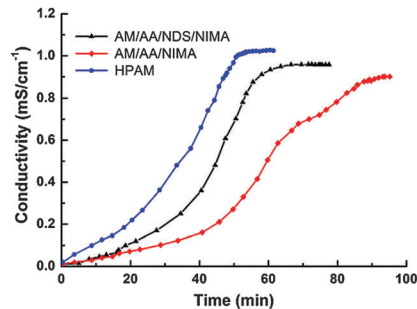


Fig. 5 Curves of conductivity changes in the dissolution process of the copolymers.

declining tendency of solubility of the associating polymers. Compared with AM/AA/NIMA, furthermore, the copolymer AM/AA/NDS/NIMA exerted preferable water solubility owing to the extra introduction of a sulfonate group in the polymer molecular chain.

### Intrinsic viscosity [ $\eta$ ]

The intrinsic viscosities [ $\eta$ ] of the copolymers AM/AA/NIMA and AM/AA/NDS/NIMA were measured, which can express the molecular weight and the expanding extent of the molecular chain of copolymer. As expected, it can be readily derived that the intrinsic viscosity of the copolymers AM/AA/NIMA and AM/AA/NDS/NIMA were  $1149.6 \text{ mL g}^{-1}$  and  $1021.8 \text{ mL g}^{-1}$ , respectively.

### Thermal stability

The mass loss and thermal gravimetric curves of AM/AA/NIMA and AM/AA/NDS/NIMA are depicted in Fig. 6. It was evident that the polymers had three stages of mass loss as the curves delineated. The first step of mass loss of AM/AA/NIMA appeared

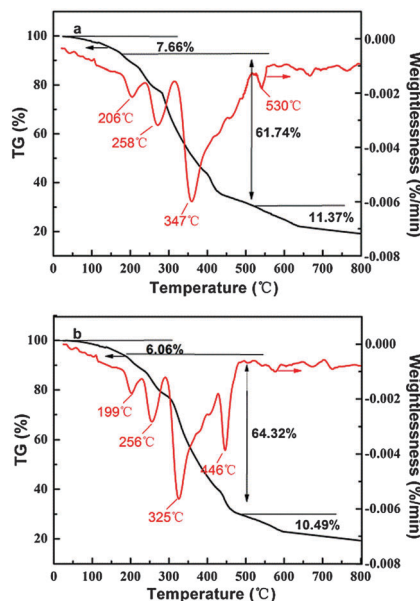


Fig. 6 Mass loss and thermal gravimetric curves of (a) AM/AA/NIMA and (b) AM/AA/NDS/NIMA.

in the range of 25–176 °C with a weight loss of 7.66 wt% owing to the evaporation of intra and intermolecular moisture, which took place in the range of 25–178 °C with a mass loss of 6.06 wt% for AM/AA/NDS/NIMA. The second one of AM/AA/NIMA occurred in the temperature range of 176–517 °C with a mass loss of 61.74%, which could be associated with the imine reaction of the amide group, and the thermolysis of the hydrophobic long chain and imidazoline ring, while that of AM/AA/NDS/NIMA appeared in the range of 178–484 °C with a weight loss of 64.31 wt%. The final stage of mass loss of AM/AA/NIMA appeared above 517 °C with the mass loss corresponding to the carbonization, whereas that of AM/AA/NDS/NIMA occurred beyond 484 °C with a mass loss of 10.49 wt%. Obviously, an excess weight loss peak of the DTG curve of AM/AA/NDS/NIMA at the second stage (446 °C) was detected in comparison with AM/AA/NIMA which can be attributed to decomposition of the sulfonate group of NDS. Furthermore, it could be observed that the mass loss rate and weight loss of AM/AA/NDS/NIMA were less than those of AM/AA/NIMA comparing the DTG curves of the obtained polymers. The thermal gravimetric data indicated that the copolymers had excellent thermal stability.

### Rheological behavior

**Shear resistance.** The conventional water-soluble polymer is sensitive to the shear degradation of viscosity at a high pressure and high flow rate, which would affect immensely its oilfield application for EOR. Depicted in Fig. 7 are the dependencies of the shear rate on the apparent viscosity of the obtained polymers and HPAM solutions at a range of certain conditions.

The results of the study of the shear stability of the synthesized copolymers in deionized water (2000 mg L<sup>-1</sup>) are delineated in Fig. 7(a). Although a sharp decrease in viscosity accompanied the shear rate rising, the trend of the decline in the apparent viscosity of the obtained polymers decreased gradually under high shear stress in comparison to HPAM. The results for the copolymers AM/AA/NIMA and AM/AA/NDS/NIMA demonstrated their excellent anti-shear degradation. The obtained higher viscosity retention rates were about 5.02% and 7.65% at 1000 s<sup>-1</sup>, respectively, compared to the HPAM solution which lost most of the viscosity, while the addition of functional monomers was maintained at an ultralow value.

To gain further insight into the anti-shear behavior, shown in Fig. 7(b) are the shear rheological results of the polymer

solutions (2000 mg L<sup>-1</sup>) in synthetic brine (see Table S1, ESI†) at 30 °C. Both of the apparent viscosity curves exhibited a small rise initially at low shear rates, but then shear thinning was observed at a high shear rate. The phenomena might be attributed to the balance of intra and intermolecular associations which could slightly increase the viscosity at a low shear rate, then the disruption and breakage of the network junction followed by the further increase in shear rate.<sup>43,44</sup> It could be concluded that the copolymers exhibited a characteristic of shear-thinning behaviour, which was attributed to the physical reversibility of the association framework.<sup>45,46</sup>

For polymers AM/AA/NIMA and AM/AA/NDS/NIMA in the aqueous phase (2000 mg L<sup>-1</sup>), the results of an extremely abrupt change in the shear rate after a permanent shear rate was applied for 5 min are shown in Fig. 7(c). It was discovered that the apparent viscosity of the polymer solutions practically underwent a flipping back and forth with the shear rate ranging from 170 s<sup>-1</sup> to 510 s<sup>-1</sup>, then back again to 170 s<sup>-1</sup>. Although a slight decline in viscosity occurred at a higher shear rate on account of the part disruption of the network structure, the obtained polymers exhibited satisfying shear stability. As the shear rate and shear stress increased however, the three-dimensional network structures of the polymer chains formed due to the intermolecular association effect are more likely to give rise to high-shear resistance.

**Temperature tolerance.** For a polymer concentration of 2000 mg L<sup>-1</sup> in the aqueous phase, an almost temperature dependent viscosity was observed at a constant shear rate, as shown in Fig. 8(a). At low temperature, an inconspicuous decrease in viscosity was initially observed, which can be attributed to the intermolecular assemblies of the polymers modified with hydrophobic groups. With the temperature rising, the progressive rupture of the intermolecular aggregation of the network structure would affect the molecular weight of the polymer, and hence lead to a decrease in solution viscosity. The AM/AA/NIMA and AM/AA/NDS/NIMA solutions displayed high temperature tolerance at 110 °C compared with that at 25 °C, and had viscosity retention rates of 40.5% and 54.8%, respectively. This could be explained by the hydrophobic effect of NIMA and the stiff microstructure of the imidazoline ring, and/or the ability of NDS to undergo strong hydrogen-bonding,<sup>47</sup> which could sustain a higher viscosity retention rate under high-temperature.<sup>48</sup>

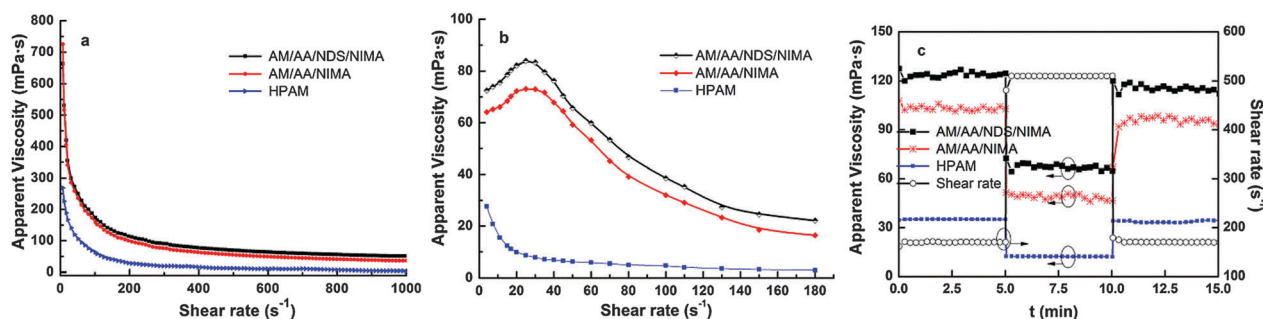


Fig. 7 Effect of shear rate on apparent viscosity in (a) aqueous phase and (b) synthetic brine; (c) shear recovery at different shear rates.

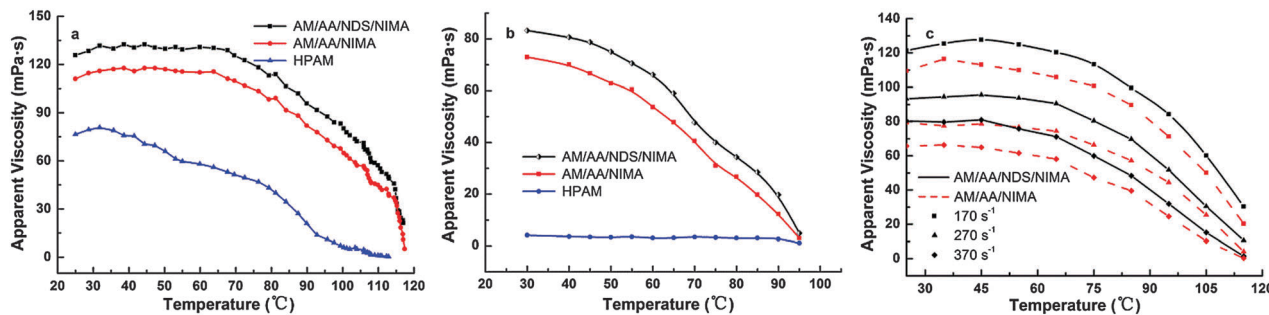


Fig. 8 Effect of temperature on the apparent viscosity in (a) the aqueous phase and (b) synthetic brine; (c) temperature tolerance at different shear rates.

Fig. 8(b) is shown to gain further insight into the temperature resistance of the obtained copolymer solutions ( $2000 \text{ mg L}^{-1}$ ) in synthetic brine (see Table S1, ESI†) at  $170 \text{ s}^{-1}$ . It could be observed that the apparent viscosity of both the synthesized polymer solutions was almost stable initially, but then decreased gradually with the temperature rising. However, a distinct difference could be easily observed when comparing the two curves, where AM/AA/NDS/NIMA presented a better viscosity retention rate (about 23.7%) than AM/AA/NIMA (about 16.9%) under the temperature of  $90 \text{ }^\circ\text{C}$ . The phenomena can be explained with the fact that incorporating electronic charges and hydrophobic groups into a water-soluble polymer can control the interaction of the intra and intermolecular interactions between the polymer chains and increase their stability in brine, which makes the apparent viscosity of the corresponding solutions less sensitive to the external temperature.<sup>49</sup>

The influence of the temperature on the copolymer solutions ( $2000 \text{ mg L}^{-1}$ ) in deionized water was investigated at range of  $25\text{--}120 \text{ }^\circ\text{C}$  at three different shear rates ( $170 \text{ s}^{-1}$ ,  $270 \text{ s}^{-1}$  and  $370 \text{ s}^{-1}$ , respectively), as shown in Fig. 8(c). As expected, it can be observed that the apparent viscosity gradually decreased with the increase in shear rate and temperature from those curves for the polymer solutions. Besides, the influence of the temperature was more prominent at a higher shear rate where the disruption of the intermolecular association effect is more pronounced compared to that at a low shear rate. The phenomena can be explained by the weakening of the hydrophobic effect at high temperature, which can lead to the increased mobility of the polymer chain and the loss of interchain interactions as the temperature increases.<sup>50</sup>

### Salt resistance

Fig. 9(a) shows the stability of the obtained copolymers at  $1000 \text{ mg L}^{-1}$  against  $\text{Na}^+$ , and the tests of resistance against  $\text{Ca}^{2+}$  or  $\text{Mg}^{2+}$  are shown in Fig. 9(b). The viscosity residual rate for the copolymer AM/AA/NIMA and AM/AA/NDS/NIMA solutions could be up to 17.1% and 10.2% in  $10\,000 \text{ mg L}^{-1}$  of NaCl solution, and then up to 12.1% and 9.3% in  $2000 \text{ mg L}^{-1}$   $\text{CaCl}_2$ , and 16.3% and 12.4% in  $2000 \text{ mg L}^{-1}$   $\text{MgCl}_2$ , respectively. Compared with HPAM, the copolymers present remarkable salt tolerance owing to the interaction of the long carbon chain of NIMA and the enhanced internal rotation resistance relating to the sulfonate groups.<sup>51</sup> Additionally, these results also demonstrated that the copolymers have preferable salt-resistance to monovalent salt than divalent salt.

### Viscoelasticity

The viscoelastic properties as a function of the oscillation frequency for copolymer AM/AA/NIMA and AM/AA/NDS/NIMA solutions ( $2000 \text{ mg L}^{-1}$ ) were researched using a Haake RheoStress 6000 rotational rheometer. The variation of the dynamic system was curved by the slope of the storage modulus  $G'$ , the loss modulus  $G''$  and the crossing point  $G_c$ , which were dependent on frequency (see Fig. 10). As indicated in Fig. 10, thereby, a viscous behavior was observed when  $G'$  was less than  $G''$  in the course of the low-frequency region. Then  $G'$  and  $G''$  increased gradually accompanying the rise in the oscillation frequency, and the elastic behavior predominated once the  $G'$  value surpassed the  $G''$  value, namely, was above the frequency at which the curves cross each other,  $G_c$ . This shows great

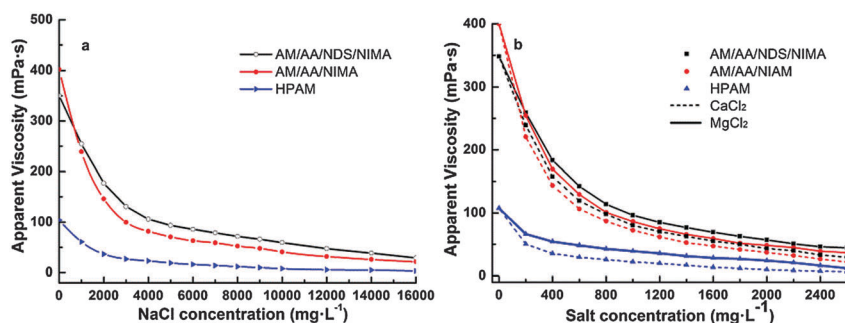


Fig. 9 Variation of the apparent viscosities of copolymer solutions with different (a) NaCl and (b)  $\text{CaCl}_2/\text{MgCl}_2$  concentrations.

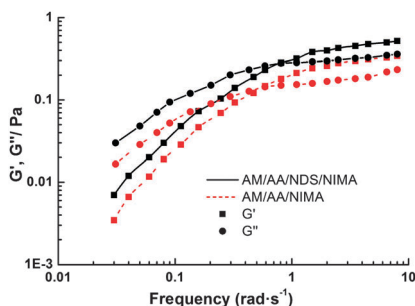


Fig. 10 Variation of viscoelastic properties with the oscillation frequency for copolymer solutions.

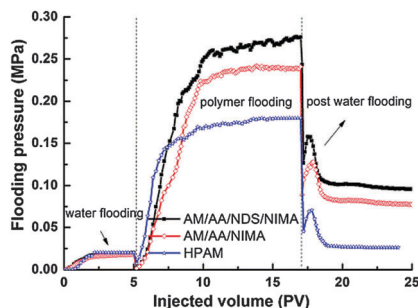


Fig. 11 Effect of injected volume on the flooding pressure.

potential for enhanced oil recovery in EOR applications attributed to the typical viscoelastic behaviour of the HAPAM solutions.<sup>52</sup>

### Core flooding analysis

**Profile control ability.** Depicted in Fig. 11 is the flooding pressure profile as function of the injected volume (PV) for 2000 mg L<sup>-1</sup> copolymer solutions and post water flooding. From the curves, it can be observed that the climbing flooding pressure presented three types of change trend, thereof the pressure increased along with the increased flooding pressure differential during the injection of polymer solutions. The flooding pressure was raised gradually at the onset of polymer flooding after 5 PV of water flooding. It can be recognized that the pressure was further increased, whereas it declined rapidly to a platform value in the wake of the injection of post water flooding. Polymer particles try to enter larger porous channels associated with their physical selection and afterwards further migrate and start to accumulate which gives rise to the injection pressure elevation and the facilitating of the post water flooding diversion. Moreover, resistance to restrain their motion would occur, while more polymer solution migrated

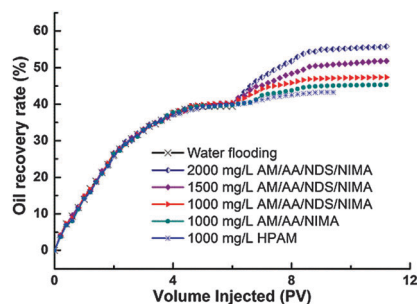


Fig. 12 Results of the core-flooding experiments.

into the porous medium as the flooding pressure and injection pressure differential was constantly elevated. Obviously, the profile control abilities of the obtained polymers were more prominent than those of HPAM, which was elucidated by the curves of flooding pressure as a function of injected volume.

Shown in Table 2 are the characteristic parameters for the polymer solution samples deduced by the core flooding experiments, such as initial flooding pressure, breakthrough pressure, stable pressure, resistance factor (RF), and residual resistance factor (RRF). Apparently, it can be observed that the two copolymers containing hydrophobic side chains exhibited superior profile control capability, whereby AM/AA/NDS/NIMA had preferable potential in the profile controlled application for enhanced oil recovery, which was associated with its higher stable flooding pressure region in comparison to AM/AA/NIMA and HPAM solutions.

**Enhanced oil recovery.** The results for the AM/AA/NDS/NIMA solution in the core flooding tests were investigated under the simulated salinity oil reservoir environment, as shown in Fig. 12. Compared with HPAM (EOR of 1000 mg L<sup>-1</sup> solution = 3.29%), the values of the obtained polymer solutions for EOR were up to 7.04% (1000 mg L<sup>-1</sup>) and 11.52% (1500 mg L<sup>-1</sup>), respectively. It was conspicuous that the value of about 15.46% more oil recovery could be obtained by the AM/AA/NDS/NIMA solution (2000 mg L<sup>-1</sup>) after water flooding. Furthermore, it was obviously discovered that the EOR effect of AM/AA/NDS/NIMA was much better than that of AM/AA/NIMA at the same concentration in the water phase.

## Conclusions

Novel imidazoline derivatives with/without sulfonate have been successfully synthesized and introduced into polyacrylamide chains *via* simple free-radical co-polymerization. The critical

Table 2 Characteristic parameters in core-flooding experiments

Core samples	Core parameter				Polymer solution samples	Pressure parameter/MPa			Residual resistance factor	
	Diameter/cm	Length/cm	Permeability/10 <sup>-2</sup> μm <sup>2</sup>	Porosity/%		Initial pressure	Breakthrough pressure	Stable pressure		
1	2.501	50.04	7.840	23.60	AM/AA/NIMA	0.0185	0.2411	0.0773	13.03	4.18
2	2.498	50.02	7.838	23.59	AM/AA/NDS/NIMA	0.0199	0.2723	0.0956	13.68	4.80
3	2.503	49.98	7.841	23.62	HPAM	0.0201	0.0705	0.0263	3.51	1.31

association concentrations of the synthetic polymers due to the dynamic transformation between intra and intermolecular junctions were in the vicinity of 0.8 g L<sup>-1</sup> and 1.0 g L<sup>-1</sup>, respectively, suggestive of the hydrophobic microdomain aggregation. The high thermostability of the terpolymer and quadri-polymer showed that the viscosity residual rates were up to 40.5% and 54.8% at 110 °C in comparison to that at 25 °C, respectively. The polymers also exhibited excellent water solubility, shear thinning (residual viscosity of 50.7 mPa s and 36.4 mPa s at 1000 s<sup>-1</sup>), shear recovery and salt resistance. The results of the core flooding tests revealed that the polymer solutions had stronger mobility control abilities and improved effective oil recovery. The above outstanding features inferred that the obtained polymers have potential technological application in high-temperature and high salinity oil recovery or other commercial applications.

## Acknowledgements

The work was financially supported by the Foundation of Youth Science and Technology Innovation Team of Sichuan Province (2015TD0007), Sichuan Provincial Science and Technology Department (13TD0025), and the Scientific Research Starting Project of Southwest Petroleum University (2014PYZ008). The authors express their sincere thanks to the financial supporters.

## Notes and references

- Q. Chen, Y. Wang, Z. Lu and Y. Feng, *Polym. Bull.*, 2013, **70**, 391–401.
- C. Zou, T. Gu, P. Xiao, T. Ge, M. Wang and K. Wang, *Ind. Eng. Chem. Res.*, 2014, **53**, 7570–7578.
- C. Zhong, P. Luo, Z. Ye and H. Chen, *Polym. Bull.*, 2009, **62**, 79–89.
- C. Chelaru, I. Diaconu and I. Simionescu, *Polym. Bull.*, 1998, **40**, 757–764.
- J. Hou, *J. Pet. Sci. Eng.*, 2007, **59**, 321–332.
- W. Kulicke, R. Kniewske and J. Klein, *Prog. Polym. Sci.*, 1982, **8**, 373–468.
- W. M. Leung, D. E. Axelson and J. D. Van Dyke, *J. Polym. Sci., Part A: Polym. Chem.*, 1987, **25**, 1825–1846.
- A. Sabhapondit, A. Borthakur and I. Haque, *J. Appl. Polym. Sci.*, 2003, **87**, 1869–1878.
- H. Kheradmand, J. François and V. Plazenet, *Polymer*, 1988, **29**, 860–870.
- R. S. Seright, J. M. Scheult and T. Talashek, *SPE Reservoir Eval. Eng.*, 2009, **12**, 783–792.
- S. E. Morgan and C. L. McCormick, *Prog. Polym. Sci.*, 1990, **15**, 103–145.
- Y. Guo, J. Liu, X. Zhang, R. Feng, H. Li, J. Zhang, X. Lv and P. Luo, *Energy Fuels*, 2012, **26**, 2116–2123.
- A. C. Lara-Ceniceros, C. Rivera-Vallejo and E. J. Jiménez-Regalado, *Polym. Bull.*, 2007, **58**, 425–433.
- T. Wan, C. Zou, L. Chen, Z. Zhou, M. Xu, W. Cheng and R. Li, *J. Solution Chem.*, 2014, **43**, 1947–1962.
- G. O. Yahaya, A. A. Ahdab, S. A. Ali, B. F. Abu-Sharkh and E. Z. Hamad, *Polymer*, 2001, **42**, 3363–3372.
- K. C. Taylor and H. A. Nasr-El-Din, *J. Pet. Sci. Eng.*, 1998, **19**, 265–280.
- S. Biggs, A. Hill, J. Selb and F. Candau, *J. Phys. Chem.*, 1992, **96**, 1505–1511.
- I. Iliopoulos, T. K. Wang and R. Audebert, *Langmuir*, 1991, **7**, 617–619.
- Y. Kakizawa, H. Sakai, K. Nishiyama, M. Abe, H. Shoji, Y. Kondo and N. Yoshino, *Langmuir*, 1996, **12**, 921–924.
- B. F. Abu Sharkh, G. O. Yahaya, S. A. Ali and I. W. Kazi, *J. Appl. Polym. Sci.*, 2001, **82**, 467–476.
- H. A. Nasr-El-Din, B. F. Hawkins and K. A. Green, Document ID: SPE-21028-MS, 20–22 February, 1991.
- N. Hameed, J. Liu and Q. Guo, *Macromolecules*, 2008, **41**, 7596–7605.
- Y. Wang, Y. Dai, L. Zhang, L. Luo, Y. Chu, S. Zhao, M. Li, E. Wang and J. Yu, *Macromolecules*, 2004, **37**, 2930–2937.
- S. Vossoughi, *J. Pet. Sci. Eng.*, 2000, **26**, 199–209.
- Y. Feng, L. Billon, B. Grassl, G. Bastiat, O. Borisov and J. François, *Polymer*, 2005, **46**, 9283–9295.
- Z. Guozhong, X. Minghui, L. Min, W. U. Huaxiao, L. Xiangli and Y. U. Peiqing, *Chin. J. Chem. Eng.*, 2010, **18**, 170–174.
- S. W. Shalaby, C. L. McCormick and G. B. Butler, *Water-soluble polymers: synthesis, solution properties, and applications*, American Chemical Society, 1991.
- P. M. Budd, *Spec. Publ. - R. Soc. Chem.*, 1996, **186**, 1–9.
- K. C. Taylor and H. A. Nasr-El-Din, *J. Pet. Sci. Eng.*, 1998, **19**, 265–280.
- R. J. English, J. H. Laurer, R. J. Spontak and S. A. Khan, *Ind. Eng. Chem. Res.*, 2002, **41**, 6425–6435.
- P. Kujawa, J. M. Rosiak, J. Selb and F. Candau, *Macromol. Chem. Phys.*, 2001, **202**, 1384–1397.
- K. Inomata, R. Doi, E. Yamada, H. Sugimoto and E. Nakanishi, *Colloid Polym. Sci.*, 2007, **285**, 1129–1137.
- K. D. Branham, G. S. Shafer, C. E. Hoyle and C. L. McCormick, *Macromolecules*, 1995, **28**, 6175–6182.
- X. Xie and T. E. Hogen-Esch, *Macromolecules*, 1996, **29**, 1734–1745.
- S. Gou, T. Yin, Z. Ye, W. Jiang, C. Yang, Y. Ma, M. Feng and Q. Xia, *J. Appl. Polym. Sci.*, 2014, **131**, 40727.
- A. Sabhapondit, A. Borthakur and I. Haque, *Energy Fuels*, 2003, **17**, 683–688.
- A. Sabhapondit, A. Borthakur and I. Haque, *J. Appl. Polym. Sci.*, 2003, **87**, 1869–1878.
- D. Wang, C. G. Williams, Q. Li, B. Sharma and J. H. Elisseeff, *Biomaterials*, 2003, **24**, 3969–3980.
- V. A. Vasantha, S. Jana, A. Parthiban and J. G. Vancso, *Chem. Commun.*, 2014, **50**, 46–48.
- E. E. Kathmann, L. A. White and C. L. McCormick, *Macromolecules*, 1997, **30**, 5297–5304.
- J. Huang, X. Li and Q. Guo, *Eur. Polym. J.*, 1997, **33**, 659–665.
- B. Gao, H. Guo, J. Wang and Y. Zhang, *Macromolecules*, 2008, **41**, 2890–2897.
- Y. Chang and C. L. McCormick, *Macromolecules*, 1993, **26**, 6121–6126.

- 44 E. Volpert, J. Selb and F. Candau, *Polymer*, 1998, **39**, 1025–1033.
- 45 I. Nahringerbauer, *J. Colloid Interface Sci.*, 1995, **176**, 318–328.
- 46 I. Nahringerbauer, *Langmuir*, 1997, **13**, 2242–2249.
- 47 S. Zheng, Q. Guo and M. Mi, *J. Polym. Sci., Part B: Polym. Phys.*, 1998, **36**, 2291–2300.
- 48 M. Rashidi, A. M. Blokhuis and A. Skauge, *J. Appl. Polym. Sci.*, 2011, **119**, 3623–3629.
- 49 E. E. Tucker, E. H. Lane and S. D. Christian, *J. Solution Chem.*, 1981, **10**, 1–20.
- 50 B. F. Abu Sharkh, G. O. Yahaya, S. A. Ali, E. Z. Hamad and I. M. Abu Reesh, *J. Appl. Polym. Sci.*, 2003, **89**, 2290–2300.
- 51 M. Rashidi, A. M. Blokhuis and A. Skauge, *J. Appl. Polym. Sci.*, 2010, **117**, 1551–1557.
- 52 Z. Ye, M. Feng, S. Gou, M. Liu, Z. Huang and T. Liu, *J. Appl. Polym. Sci.*, 2013, **130**, 2901–2911.